

Published in final edited form as:

*Circ Res.* 2016 September 30; 119(8): 909–920. doi:10.1161/CIRCRESAHA.116.309202.

## A Simplified, Langendorff-Free Method for Concomitant Isolation of Viable Cardiac Myocytes and Nonmyocytes From the Adult Mouse Heart

**Matthew Ackers-Johnson** and

Cardiovascular Research Institute, Centre for Translational Medicine MD6, National University Health System, Singapore; Genome Institute of Singapore

**Peter Yiqing Li**

Cardiovascular Research Institute, Centre for Translational Medicine MD6, National University Health System, Singapore

**Andrew P. Holmes, Sian-Marie O'Brien, and Davor Pavlovic**

Institute of Cardiovascular Sciences, University of Birmingham, UK

**Roger S. Foo**

Cardiovascular Research Institute, Centre for Translational Medicine MD6, National University Health System, Singapore; Genome Institute of Singapore

### Abstract

**Rationale**—Cardiovascular disease represents a global pandemic. The advent of and recent advances in mouse genomics, epigenomics, and transgenics offer ever-greater potential for powerful avenues of research. However, progress is often constrained by unique complexities associated with the isolation of viable myocytes from the adult mouse heart. Current protocols rely on retrograde aortic perfusion using specialized Langendorff apparatus, which poses considerable logistical and technical barriers to researchers and demands extensive training investment.

**Objective**—To identify and optimize a convenient, alternative approach, allowing the robust isolation and culture of adult mouse cardiac myocytes using only common surgical and laboratory equipment.

**Methods and Results**—Cardiac myocytes were isolated with yields comparable to those in published Langendorff-based methods, using direct needle perfusion of the LV *ex vivo* and without requirement for heparin injection. Isolated myocytes can be cultured antibiotic free, with retained organized contractile and mitochondrial morphology, transcriptional signatures, calcium handling, responses to hypoxia, neurohormonal stimulation, and electric pacing, and are amenable to patch clamp and adenoviral gene transfer techniques. Furthermore, the methodology permits concurrent isolation, separation, and coculture of myocyte and nonmyocyte cardiac populations.

---

Correspondence to Dr Roger S. Foo, Cardiovascular Research Institute, Centre for Translational Medicine MD6, National University Health System, 117599 Singapore. mdcrrfsy@nus.edu.sg.

**Disclosures**

None.

**Conclusions**—We present a novel, simplified method, demonstrating concomitant isolation of viable cardiac myocytes and nonmyocytes from the same adult mouse heart. We anticipate that this new approach will expand and accelerate innovative research in the field of cardiac biology.

### Keywords

cardiac fibroblasts; cardiomyocytes; cardiovascular disease; coculture; Langendorff-free; mouse models; single-cell isolation

---

Cardiovascular disease constitutes a global pandemic.<sup>1,2</sup> Incidence of heart failure is increasing despite improvement in the understanding and management of disease, and prognosis remains poor.<sup>3</sup> Cardiac myocytes (CMs), the contractile cells of the heart, are the traditional focus of extensive research in cardiac biology. CMs coordinate rhythmic beating and integrate multiple hormonal, neural, electric, mechanical, and exosome-mediated signals through a variety of cell-surface and nuclear receptors.<sup>4,5</sup> Physiological adaptive responses may rapidly become pathological. A deeper mechanistic understanding is therefore imperative to the development of novel intervention strategies.

Myocytes in the intact adult myocardium exist in close association with neighboring cells and extracellular matrix and are highly sensitive to mechanical perturbations, enzymatic damage, hypoxia, nutrient bioavailability, pH, and ionic fluctuations. Mounting of excised hearts on Langendorff apparatus and retrograde aortic perfusion with enzyme-containing buffers was conceived over 45 years ago<sup>6,7</sup> and remains the centerpiece of every modern established protocol to date for the isolation and study of adult rodent CMs.<sup>4,8–17</sup>

However, the necessity for commercial or custom-made apparatus, and considerable expertise therewith, represents a significant financial, logistical, and technical barrier for groups wishing to engage in research using isolated adult CMs. Also, Langendorff-based approaches suffer issues with sterility and typically require preinjection of animals with anticoagulants such as heparin, which is detrimental to downstream polymerase chain reaction-based analyses.<sup>18,19</sup> Furthermore, mouse CMs are exceptionally delicate, and successful mounting of the small mouse aorta onto Langendorff apparatus is particularly challenging. These issues risk precluding the full potential for cardiac research of recent advances in mouse genomics, epigenomics, transgenics, and gene therapy.<sup>20–23</sup>

We present here a novel alternative approach to the challenge of myocyte isolation and culture from the myocardia of adult mouse hearts. We introduce 3 key modifications to standard protocols. First, hearts are rapidly perfused with a high EDTA buffer to inhibit contraction and coagulation and to destabilize extracellular connections. Second, pH of buffers is adjusted to an optimal 7.8. Third, all buffers are introduced by intraventricular injection, with deep myocardial perfusion via the coronary vasculature induced by clamping of the aorta (Figure 1). The procedure is simple, is flexible, does not require heparin injection, may be performed wholly in a sterile laminar flow cabinet, and uses surgical tools and equipment found readily in most animal laboratory facilities.

Reproducible yields are achieved in line with published Langendorff procedures of 1 million myocytes per left ventricle and  $81\pm 6\%$  viable, calcium-tolerant, rod-shaped cells.

Isolated CMs can be cultured antibiotic free, retain organized morphology and functionality, and are amenable to patch clamping and adenoviral gene transfer. The procedure is compatible with automated pump infusion systems and, furthermore, permits the concurrent isolation, culture, and coculture of mouse nonmyocyte resident cardiac populations, from the same regions, in the same heart. We anticipate that this new approach will expand and accelerate innovative research in the field of cardiac biology.

## Methods

### Isolation and Culture of CMs and Nonmyocytes From Adult Mouse Heart

A schematic overview of the myocyte isolation procedure is shown in Figure 2. An expanded description of the procedure, accompanied with images and videos, and complete materials list is available in the Online Data Supplement, alongside full details of additional methods applied in this study (Appendix A-ix). All animal work was undertaken in accordance with Singapore National Advisory Committee for Laboratory Animal Research guidelines. Relevant national and institutional guidelines and regulations must be consulted before commencement of all animal work.

Buffers and media were prepared as detailed in Appendix D. EDTA, perfusion, and collagenase buffers were apportioned into sterile 10 mL syringes, and sterile 27 G hypodermic needles were attached (Online Figure IA).

C57/BL6J mice aged 8 to 12 weeks were anesthetized, and the chest was opened to expose the heart. Descending aorta was cut, and the heart was immediately flushed by injection of 7 mL EDTA buffer into the right ventricle. Ascending aorta was clamped using Reynolds forceps, and the heart was transferred to a 60-mm dish containing fresh EDTA buffer. Digestion was achieved by sequential injection of 10 mL EDTA buffer, 3 mL perfusion buffer, and 30 to 50 mL collagenase buffer into the left ventricle (LV). Constituent chambers (atria, LV, and right ventricle) were then separated and gently pulled into 1-mm pieces using forceps. Cellular dissociation was completed by gentle trituration, and enzyme activity was inhibited by addition of 5 mL stop buffer.

Cell suspension was passed through a 100- $\mu$ m filter, and cells underwent 4 sequential rounds of gravity settling, using 3 intermediate calcium reintroduction buffers to gradually restore calcium concentration to physiological levels. The cell pellet in each round was enriched with myocytes and ultimately formed a highly pure myocyte fraction, whereas the supernatant from each round was combined to produce a fraction containing nonmyocyte cardiac populations.

CM yields and percentage of viable rod-shaped cells were quantified using a hemocytometer. Where required, the CMs were resuspended in prewarmed plating media and plated at an applicationdependent density, onto laminin (5  $\mu$ g/mL) precoated tissue culture plastic or glass coverslips, in a humidified tissue culture incubator (37°C, 5% CO<sub>2</sub>). After 1 hour, and every 48 hours thereafter, media was changed to fresh, prewarmed culture media.

The cardiac nonmyocyte fraction was collected by centrifugation (300g, 5 minutes), resuspended in fibroblast growth media, and plated on tissue-culture treated plastic, area  $\approx$  23 cm<sup>2</sup> (0.5 $\times$  12-well plate) per LV, in a humidified tissue culture incubator. Media was changed after 24 hours and every 48 hours thereafter.

## Results

### Langendorff-Free Isolation of CMs From the Adult Mouse Heart

Cannulation and retrograde perfusion of the aorta, to force dissociation buffers deep into the myocardium via the coronary vasculature, is the cornerstone of all widely adopted protocols for myocyte isolation from the adult mouse heart. We hypothesized that the same hydrodynamic effect could be achieved in a much simplified manner, by clamping the aorta, and injecting buffers directly into the LV (Figure 1). We further supposed that because of the increased ease and speed of this procedure, preinjection of mice with anticoagulants such as heparin could be avoided and replaced by preclearing of heart chambers using the divalent cation chelating agent EDTA. Thus, the basis of methodology outlined in (Figure 2) was formed.

For each experiment, crude digestion product was monitored, and total cell number and percentage of viable rodshaped myocytes were subsequently quantified using a hemocytometer (Figure 3A). After calcium reintroduction, myocytes remained quiescent and adhered to laminin-coated culture surfaces, displaying characteristic angular morphology and clearly organized sarcomeric striation patterns (Figure 3B and 3C). Optimal rod-shaped yields were most reliably achieved at dissociation buffer pH 7.8 and using a high preclearing buffer EDTA concentration of 5 mmol/L (Figure 3D and 3E; Online Figure IIA and IIB). With these conditions, the protocol reproducibly yields 1 million myocytes per LV and 81 $\pm$ 6% viable, rod-shaped cells. This is in line with yields reported previously in established Langendorff-based protocols.<sup>9,10,12,15</sup> Furthermore, the protocol was found to be compatible with automated infusion pumps for controlled delivery of injected digestion buffers. Flow rates of 1 to 5 mL/min all produced average yields of over 60% rod-shaped cells, demonstrating robustness of methodology, whereas the highest total cell yields were achieved at 1 mL/min (Online Figure IIC).

### Morphology and Culture of Isolated LV CMs

We next explored the optimal conditions for maintaining viable CMs in culture. Several varieties of basal media were initially tested as components of culture media for their ability to support the preserved morphology of plated LV myocytes for a period of 4 days, and medium 199 was selected, in line with some previous reports<sup>14</sup> (Online Figure IID). pH is a variable known to critically influence behavior of myocytes in culture, with some laboratories opting for neutral or even slightly acidic pH 6.9 to 7.0.<sup>9,10,12</sup> Experiments were therefore performed to test cell morphology and viability in a carefully controlled pH range of 6.7 to 7.9, as described in Methods (Online Appendix A-ix). Indeed, we observed that myocytes cultured at reduced pH best retained their rod-shaped morphology and were resistant to remodeling even in the presence of 10% fetal bovine serum (Online Figure IID). However, we also discovered that while rod-shaped morphology is traditionally equated with

cell viability, this is not necessarily the case, particularly after extended time in culture. Application of the nuclear ethidium homodimer stain, which is excluded from viable cells, to myocytes after 7-day culture at pH 6.7 revealed that large numbers of rod-shaped cells were in fact nonviable (Online Figure IID). This was not the case for myocytes cultured at pH 7.4, and furthermore, many of the cells that had not retained their rod shape at pH 7.4, nonetheless, remained viable. We therefore highlight an important distinction between remodeling and viability and suggest that although culturing at reduced pH can suppress myocyte remodeling and retain differentiated morphological characteristics, such conditions are in fact detrimental to cell viability in long-term culture. With this in consideration, we proceeded to separately quantify both rod-shaped morphology and viability for 7 days in culture with a pH range of 6.7 to 7.9. Indeed, although there was little improvement in cell morphology (Figure 3F), there was a marked preservation of cell viability at pH 7.4 beyond 3 days in culture (Figure 3G).

Adult myocytes exhibit a metabolic preference for fatty acid oxidation as an energy source.<sup>24</sup> We therefore tested media supplementation with a defined lipid mixture and observed further improvement in viability to the extent that 60% of initially adhered myocytes remained viable after 7 days in culture (Figure 3H and 3I). Given concerns that lipid and insulin constituents of culture medium could interfere with metabolic assays, it is noteworthy that cell viability without either of these additives remained above 40% (Online Figure IIG). Interestingly, insulin supplementation demonstrated clear improvements in viability only in lower pH range cultures. However, inclusion may still elicit functional benefits at pH 7.4.<sup>25</sup> Media supplementation with 5 mmol/L taurine, creatine, adenosine, and inosine<sup>26–29</sup> was additionally tested but had little beneficial effect (data not shown).

Progressive, active remodeling of adult CMs in culture is well documented.<sup>14,30,31</sup> Concordantly, the angular morphology and ordered sarcomeric arrangements of plated myocytes remained largely intact after 24-hour culture (Figure 3J and Online Movie III), but cell edges began to round after 2 to 3 days, and organized sarcomeric patterning was typically lost by day 7. Continued culture produced cells with distinctive emerging pseudopodia, and beyond 8 days, some cells seemed to re-establish organized contractile apparatus, beat spontaneously, or form contacts with neighboring cells and contract in synchrony. This phenomenon was accelerated by addition of 10% fetal bovine serum and removal of 2,3-butanedione monoxime and bears resemblance to dated redifferentiation techniques.<sup>8,32</sup>

### **Cultured Myocytes Are Intact, Retain Transcriptional and Functional Characteristics, and Are Amenable to Investigative Techniques**

The process of isolating adult CMs carries an inherent risk of causing cellular damage or activation of stress response pathways that could potentially confound *in vivo* or downstream transcriptional profiles. To test the integrity of the plasma membranes of freshly plated myocytes, a live/dead dual viability stain was used. Myocytes were clearly able to de-esterify and retain calcein AM (green) fluorescent dye, while excluding ethidium homodimer (red) nuclear stain, demonstrating intact, viable cells (Figure 4A). Peroxide-induced cell death led to loss of calcein retention and gain of ethidium homodimer staining.

Pressure overload of adult hearts induces myocyte hypertrophy, which is associated with increased expression of markers including natriuretic peptides ANP (*Nppa*) and BNP (*Nppb*) and the skeletal isoform of  $\alpha$ -actin (*Acta1*).<sup>33</sup> To examine the conservation of these stress-associated transcriptional signatures, myocytes were isolated from transverse aortic constriction–operated mouse hearts, 8 weeks postoperation, alongside sham-operated controls. Yields of viable rodshaped myocytes dropped to  $65\pm 15\%$  from transverse aortic constriction–operated hearts (data not shown), likely because of the pathological hypertrophic phenotype,<sup>34</sup> although this is still well within the limits of successful myocyte isolations in established protocols. Despite this, quantitative polymerase chain reaction of myocytes isolated from both left and right ventricles revealed the preservation of increased transcriptional stress signatures in transverse aortic constriction–operated hearts, versus sham-operated controls (Figure 4B).

Transcriptional stress response, calcium handling, contractility, electric potential, and amenability to adenoviral transduction were next tested in freshly plated cells from healthy hearts to confirm applicability of isolated myocytes to scientific investigation. Hypoxic stress was induced by 24-hour incubation in a chamber under a controlled nitrogen atmosphere containing 5% CO<sub>2</sub> and 0.2% O<sub>2</sub>. Cells were then analyzed for expression of hypoxia-responsive genes. Significant increases in expression of *Nppa*, *Nppb*, fetal isoform myosin heavy chain (*Myh7*), glucose transporter (*Slc2a1*), and metabolism-related hexokinase (*Hk2*) genes, but not mitochondrial biogenesis–related MAX interactor 1 (*Mxi1*), were strongly upregulated after hypoxic exposure<sup>33,35</sup> (Figure 4C).

To demonstrate the suitability of preparations for biochemical signaling experiments, plated myocytes were challenged with varying doses of adrenergic activators norepinephrine and isoproterenol. Lysates were subsequently analyzed by Western blotting with specific antibodies to detect phosphorylation of protein kinase B (AKT), phospholamban, and extracellular signal–related kinase. Both stimuli elicited dose-dependent increases in AKT and phospholamban phosphorylation (Figure 4D). AKT phosphorylation was also observed to increase with increased norepinephrine incubation time 20 minutes, whereas phospholamban phosphorylation saturated within 1 minute, and extracellular signal–related kinase exhibited somewhat fluctuating increases in phosphorylation over time (Online Figure III).

After removal of 2,3-butanedione monoxime from culture medium, plated myocytes exhibited spontaneous calcium transients, which could be visualized using the calcium-sensitive fluorophore Fluo-4 AM. Signals typically emanated from one or less frequently both termini and moved steadily across the cell longitudinal axis, coinciding with waves of partial contraction (Online Figure IVA and Movie IVA and IVB). Addition of norepinephrine elicited increased rates of spontaneous calcium transient initiation, propagation, and cell contraction in individual cells, further indicating intact adrenergic signaling and response mechanisms in plated cells<sup>36</sup> (Online Figure IVB).

Additional experiments were performed to quantify calcium-handling properties and adrenergic responses in freshly isolated myocytes. Electrically paced cells exhibited characteristic frequency-dependent changes in calcium handling (Online Figure VA) and

sarcomere shortening (Online Figure VB), including reduced sarcomere shortening at higher pacing frequency, as expected.<sup>37</sup> Importantly, myocytes responded to adrenergic stimulation in a dose-dependent manner, in accordance with previous studies.<sup>38</sup> Administration of isoproterenol amplified both calcium transients and sarcomere length shortening (Figure 4E). Specifically, increasing doses of isoproterenol stimulated increased calcium transient amplitude (Figure 4F), decreased calcium decay constant ( $\tau$ ) (Figure 4G), and increased sarcomere length shortening (Figure 4H). Representative individual pre- and postisoproterenol calcium transient and sarcomere length traces are shown in Online Figure VC and VD. A normalized calcium transient trace is shown to highlight the reduced transient decay time in the presence of isoproterenol.

To confirm the amenability of isolated CMs to patch clamp studies, sodium current ( $I_{Na}$ ) was quantified in freshly isolated myocytes. Measurements of whole cell  $I_{Na}$  from single myocytes under voltage clamp mode could be readily evoked in all cells tested, with the peak  $I_{Na}$  current density measuring  $-36\pm 3$  pA/pF at a test potential of  $-40$  mV.  $I_{Na}$  displayed robust voltage dependence with a mean  $V_{0.5}$  of  $-52\pm 1$  mV and reverse potential of  $8\pm 2$  mV (Figure 5A and 5B). These values are consistent with previous reports of rodent ventricular  $I_{Na}$  measured under similar conditions.<sup>39,40</sup> The steady-state inactivation (availability) of  $I_{Na}$  exhibited voltage dependency with a mean  $V_{0.5}$  of  $-86\pm 1$  mV (Figure 5C and 5D), again in keeping with previously recorded data.<sup>39,40</sup> Thus, the magnitude of  $I_{Na}$  and the activation and inactivation kinetics of  $I_{Na}$  are measurably preserved using this isolation technique.

Healthy adult CMs contain dense, highly organized networks of mitochondria running parallel to sarcomeres in the cell longitudinal axis, which have key roles in cell bioenergetics and in injury or disease.<sup>24,32,41,42</sup> To visualize active mitochondria in cultured myocytes, cells were loaded with membrane potential-dependent MitoTracker Red CMXRos dye and analyzed by confocal microscopy. The characteristic mitochondrial network patterning of healthy myocytes was confirmed in our cells (Online Figure VI).

Experiments using cultured cells often require the manipulation of endogenous or exogenous nucleic acids. Adenoviral vectors are an effective tool for introduction of expression constructs into CMs.<sup>9,13,14,43</sup> To test myocyte transduction capability in the current procedure, cells were treated with adenoviral expression constructs encoding the myogenic transcriptional coactivator myocardin (Ad5.Myocd), dominantnegative Myocd-DN (Ad5.Myocd-DN), or GFP control (Ad5. GFP). Myocd-DN encodes a truncated form of myocardin that competes with endogenous myocardin for binding at target gene promoters but lacks a C-terminal transcription-activating domain.<sup>44</sup> Subsequent analysis of gene expression demonstrated that Ad5.Myocd treatment caused significant 4-fold and 2-fold upregulation of myocardin target genes *Nppa* and *Nppb*,<sup>45</sup> respectively, whereas expression was strongly suppressed by treatment with Ad5.Myocd-DN. Phenylephrine treatment further increased *Nppa* although not *Nppb* expression in control and Ad5.Myocd-treated myocytes, but this increase was abrogated in Ad5.Myocd-DN-treated myocytes (Online Figure VII). Thus, the current protocol is well suited for studies involving adenoviral mediated gene transfer, expression, and responses in cultured adult mouse CMs.

## Concurrent Isolation and Culture of CMs and Fibroblasts From a Single Mouse Heart

The mammalian adult heart contains substantial populations of nonmyocyte cells, with emerging roles in cardiac physiology, pathology, and regenerative capacity.<sup>46–48</sup> Cardiac fibroblasts (CF) represent a sizeable albeit ill-defined population, with critical functions during health and disease.<sup>49,50</sup> There are currently no peer-reviewed published protocols describing the concomitant isolation, culture, and study of myocytes and fibroblasts from the same adult mouse heart.

Traditional protocols for CF culture involve a simple enzymatic digestion of the heart, centrifugation of crude product, and plating in serum-containing media.<sup>50</sup> We set out to test whether CFs could be cultured in a similar manner from the current nonmyocyte supernatant fractions of LV digestion products. For comparison, fibroblasts were isolated from mouse tails (tail fibroblasts [TF]) in parallel.

Cells were observed to attach and proliferate to near confluency within 4 to 5 days and were confirmed positive for the fibroblast marker vimentin by immunocytochemical staining. The absence of adhered CMs was confirmed by negative TNNT (cardiac troponin-T) staining, and conversely, absence of contaminating fibroblasts in plated CM samples was confirmed by negative vimentin staining, indicating complete separation of the 2 cellular fractions (Figure 6A).

## Cultured CFs Recapitulate Characteristics of CFs From Traditional Protocols

Cultured CFs displayed extensive morphological differences when compared with TFs, with increased cell spreading, cytoplasmic protrusions, and a distinctive asymmetrical looping shape that were particularly pronounced at subconfluent cell densities (Online Figure VIII A). It has been reported that CFs express a cardiogenic transcriptional network.<sup>50</sup> Accordingly, freshly cultured CMs, TFs, and CFs (p0), and CFs after 1 (p1) and 2 (p2) passages, were harvested for analysis of gene expression. Quantitative polymerase chain reaction data are summarized graphically as a heat map in Figure 6B. Expression of 3 selected canonical fibroblast and cardiogenic genes are also represented in standard format (Online Figure VIII B through VIII G). Detection of CM-associated genes was largely limited to myocytes. Freshly isolated CFs tended to express lower levels of canonical fibroblast marks than TFs, other than collagen synthesis genes *Colla1* and *Colla2*. Conversely, CFs showed markedly higher expression of cardiogenic associated genes than TFs, often higher also than CMs. These results are consistent with previous findings<sup>55</sup> and pave the way for easily achievable coculture experiments to study cell–cell interactions in vitro (Figure 6C). Furthermore, the cultured CFs were able to activate a transition to myofibroblasts, marked by increased production of smooth muscle  $\alpha$  actin in response to transforming growth factor  $\beta$  stimulation (Figure 6D), and this potential was retained for at least 2 passages (Figure 6E). Therefore, evidence supports the use of the current protocol for the isolation, culture, and study of CFs, in addition to CMs.

## Isolated Cardiac Nonmyocytes Represent a Heterogeneous Population

Although cultured CF reliably recapitulated characteristic observations from previous studies, close visual inspection revealed areas within cultures displaying unique



morphological features (Online Figure IXA), sometimes resembling endothelial networks (Online Figure IXB). Analysis of the nonmyocyte-containing fraction by flow cytometry using specific antibodies confirmed the presence of smooth muscle cells (ACTA2+), fibroblasts (THY1+), endothelial cells (CD146+ or positive for *Griffonia simplicifolia* isolectin-B4 staining), and immune-related cells (CD45+) (Figure 7A; Online Figure IXC).

Plated cultures were tested for the presence of endothelial cells by immunocytochemical staining against CD31. In subconfluent cultures, positive staining was detected, but limited to small, infrequent clusters (Figure 7B). However, in postconfluent cultures, CD31-positive cells marked the distinctive networks observed previously, which stained strongly for actin and negative for the fibroblast marker vimentin, leading to their positive identification as endothelial cell networks (Figure 7C and 7D). Although rarely discussed in the literature, it seems likely that CFs obtained by traditional methods would comprise a similarly heterogeneous population, which may have passed undetected, particularly when limiting studies to subconfluent cultures.<sup>50</sup> However, the identification of such cells raises the tantalizing prospect for utilization of the current protocol in simplified concurrent isolation of not only myocytes and fibroblasts but also endothelial cells and the potential array of diverse cardiac-resident nonmyocyte populations that continue to be investigated and discovered.

## Discussion

Isolated adult CMs have proven an ideal model for valuable insights into diverse aspects of cardiac physiology and pathobiology, from contractility, calcium handling, and electrophysiology, to signaling, bioenergetics, drug testing, single cell transcriptomics, and apoptosis.<sup>16,24,51–56</sup> However, progress using current protocols is often constrained by technical and logistical difficulties associated with the Langendorff-based isolation and maintenance of high yields of viable adult CMs. In this report, we present a novel, convenient approach to isolate viable, calcium-tolerant myocytes from the adult mouse heart, using only standard surgical tools and equipment and without the prerequisite of heparinization. Yields of total and viable myocytes are consistent with and sometimes exceed those reported in previous Langendorff-based procedures.<sup>9,10,12,15</sup> Furthermore, we demonstrate the concomitant isolation and culture of myocytes and nonmyocytes from the same mouse heart.

The described protocol builds on decades of international research, with buffer recipes and culture techniques adapted from work in many excellent papers and reviews.<sup>4,8–12,14,15</sup> We introduce 3 key modifications to standard protocols: preperfusion with high EDTA buffer, pH correction, and, most notably, simple intraventricular injection of all dissociation buffers.

The divalent cation chelator EDTA was first tested as a substitute for heparinization, amid some concern that EDTA may be damaging to myocytes.<sup>57,58</sup> However, a common theme of adult CM isolation procedures is the importance of initial perfusion using calcium-free buffers,<sup>59</sup> with some reports indeed using low micromolar concentrations of EDTA, or the higher calcium-affinity analogue EGTA.<sup>8,13,30,55</sup> It seems that initial chelation of divalent

cations using EDTA may impart multiple benefits, including the inhibition of blood coagulation, inhibition of CM cell contractions, and loosening of intercellular connections.<sup>7,60</sup>

Previous CM isolation methods adopt a physiological pH between 7.0 and 7.4 for dissociation buffers, generally without presenting supporting evidence. It is unclear why a pH of 7.8 seems optimal for the current protocol. Possibly, higher pH offsets acidification in cases of myocardial lactate production, increases EDTA affinity for divalent cations, or, interestingly, improves glucose utilization via increased phosphofructokinase activity, which functions at an optimum pH of 8.0.<sup>61</sup>

Introduction of dissociation buffers by intraventricular injection negates the requirement for Langendorff perfusion apparatus, simplifies, and easily facilitates the option for conducting the entire procedure in a sterile laminar flow cabinet. The heart is perfused immediately at euthanasia, and precise identification of the mouse aorta is not necessary for clamp application, substantially reducing the potential for errors, blood coagulation, ischemia, and incorrect mounting of the heart, encountered when using traditional retrograde perfusion techniques. Some previous protocols emphasize the critical importance of maintaining the perfused heart at 37 °C.<sup>55</sup> Digestion is certainly faster at 37 °C, but we do not find temperature to be a key variable affecting the number or viability of isolated myocytes and have successfully conducted isolation procedures at room temperature. The protocol is compatible with automated pump injection systems, for precise control of buffer pressure or flow rates. However, standard injection using disposable syringes is sufficient and may help ensure sterility and a higher degree of control over perfusion for individual hearts, given that marked biological variability occurs between mice even within littermate groups. Sterile procedure and antibiotic-free culture may be particularly useful for studies involving CM calcium handling or electrophysiology, given the influence of streptomycin and analogues on certain ion channel functions.<sup>62</sup>

Cultured myocytes retained characteristic morphology, transcriptional signatures, and functionality, with organized sarcomeric contractile apparatus and mitochondrial networks, calcium handling, responses to neurohormonal, electric, and hypoxic stimuli, and amenability to patch clamping and adenoviral mediated gene transfer. Progressive remodeling was observed with extended periods in culture, as noted in previous reports.<sup>14,30,31</sup> Various strategies to prevent or decelerate this process have been proposed, including addition of the bioactive molecules N-benzyl-p-toluene sulfonamide,<sup>63</sup> blebbistatin,<sup>64</sup> or cytochalasin D.<sup>30,65</sup> N-benzyl-p-toluene sulfonamide and blebbistatin are also suggested as specific myosin II ATPase inhibitors during myocyte culture to replace 2,3-butanedione monoxime, which has received some criticism for off-target bioenergetic, phosphatase, and calcium regulatory effects.<sup>64,66–68</sup> Although not tested here, such compounds may easily be incorporated into the current protocol for application-specific purposes.

Nonmyocyte cardiac populations are rapidly gaining recognition as key participants in heart biology and pathophysiology.<sup>46–48</sup> CFs were successfully cultured from the nonmyocyte fraction of ventricular digestion product and closely recapitulated previously reported

morphology and cardiogenic-like transcriptional profiles.<sup>50</sup> The presence of endothelial populations was also detected in cultures. It is unclear whether such populations exist in the fibroblast cultures of other reports. It is also likely possible, and through personal communication a practice in some laboratories, to equally isolate nonmyocytes in the same manner from adult mouse heart digestion products after Langendorff-based protocols, although this is not to our knowledge published in any peer-reviewed literature. In either case, the current report raises the exciting prospect of simplified, simultaneous isolation and profiling of a range of nonmyocyte populations, alongside viable CMs, from the same regions, in the same mouse heart.

Taken together, the described method offers a novel, convenient approach to the isolation and study of mouse CMs, removing technical and logistical obstacles posed by previous Langendorff-based techniques and opening the door to new, critical, and exciting research into both myocyte and nonmyocyte populations in the adult mouse heart.

## Supplemental Material

Refer to Web version on PubMed Central for supplementary material.

## Acknowledgments

We would like to thank Ning Ding and the SBIC-Nikon Imaging Centre, Biopolis, Singapore, for kind assistance with confocal microscopy. Also to Dr Tuan Luu for performing TAC surgery, Dr Justus Stenzig for assistance with flow cytometry, Dr Chukwuemeka George Anene-Nzeli for assistance with capturing of spontaneous calcium transient data, and Prof Paulus Kirchhof and Dr Larissa Fabritz for provision of staff and equipment for patch clamping studies.

### Sources of Funding

This work was funded by CSA (SI), Cardiovascular Centre Grant NUH, and CS-IRG from the National Medical Research Council and the Biomedical Research Council, A\*STaR, Singapore, to R.S.F., Wellcome Trust Seed Award Grant (109604/Z/15/Z) to D.P., British Heart Foundation Grant (FS/13/43/30324) to P.K. and L.F., and Leducq Foundation Grant to P.K. Equipment and staff provided by P.K. and L.F. to help with patch clamp studies, as noted in Acknowledgments, were funded through the stated grants.

## Nonstandard Abbreviations and Acronyms

<b>BSA</b>	bovine serum albumen
<b>CF</b>	cardiac fibroblast
<b>CM</b>	cardiac myocyte
<b>DAPI</b>	4',6-diamidino-2-phenylindole
<b>DMEM</b>	Dulbecco's Modified Eagle Medium
<b>EDTA</b>	ethylenediaminetetraacetic acid
<b>EGTA</b>	ethylene glycol tetraacetic acid
<b>HEPES</b>	N-2-hydroxyethylpiperazine-N'-2-ethanesulfonic acid
<b>I<sub>Na</sub></b>	sodium current

<b>LV</b>	left ventricle
<b>PBS</b>	phosphate buffered saline
<b>RV</b>	right ventricle
<b>TF</b>	tail fibroblast

## References

1. Wong ND. Epidemiological studies of CHD and the evolution of preventive cardiology. *Nat Rev Cardiol.* 2014; 11:276–289. DOI: 10.1038/nrcardio.2014.26 [PubMed: 24663092]
2. Cook C, Cole G, Asaria P, Jabbour R, Francis DP. The annual global economic burden of heart failure. *Int J Cardiol.* 2014; 171:368–376. DOI: 10.1016/j.ijcard.2013.12.028 [PubMed: 24398230]
3. Braunwald E. The war against heart failure: the Lancet lecture. *Lancet.* 2015; 385:812–824. DOI: 10.1016/S0140-6736(14)61889-4 [PubMed: 25467564]
4. Sambrano GR, Fraser I, Han H, Ni Y, O’Connell T, Yan Z, Stull JT. Navigating the signalling network in mouse cardiac myocytes. *Nature.* 2002; 420:712–714. DOI: 10.1038/nature01306 [PubMed: 12478303]
5. Cervio E, Barile L, Moccetti T, Vassalli G. Exosomes for intramyocardial intercellular communication. *Stem Cells Int.* 2015; 2015:482171.doi: 10.1155/2015/482171 [PubMed: 26089917]
6. Kono T. Roles of collagenases and other proteolytic enzymes in the dispersal of animal tissues. *Biochim Biophys Acta.* 1969; 178:397–400. [PubMed: 4306267]
7. Berry MN, Friend DS, Scheuer J. Morphology and metabolism of intact muscle cells isolated from adult rat heart. *Circ Res.* 1970; 26:679–687. [PubMed: 4316328]
8. Mitcheson JS, Hancox JC, Levi AJ. Cultured adult cardiac myocytes: future applications, culture methods, morphological and electrophysiological properties. *Cardiovasc Res.* 1998; 39:280–300. [PubMed: 9798514]
9. Zhou YY, Wang SQ, Zhu WZ, Chruscinski A, Kobilka BK, Ziman B, Wang S, Lakatta EG, Cheng H, Xiao RP. Culture and adenoviral infection of adult mouse cardiac myocytes: methods for cellular genetic physiology. *Am J Physiol Heart Circ Physiol.* 2000; 279:H429–H436. [PubMed: 10899083]
10. Alliance for Cellular Signalling (AfCS) Procedure Protocol ID PP00000125. <http://www.signaling-gateway.org/data/ProtocolLinks.html>
11. Liao R, Jain M. Isolation, culture, and functional analysis of adult mouse cardiomyocytes. *Methods Mol Med.* 2007; 139:251–262. [PubMed: 18287677]
12. O’Connell TD, Rodrigo MC, Simpson PC. Isolation and culture of adult mouse cardiac myocytes. *Methods Mol Biol.* 2007; 357:271–296. DOI: 10.1385/1-59745-214-9:271 [PubMed: 17172694]
13. Kaestner L, Scholz A, Hammer K, Vecerde A, Ruppenthal S, Lipp P. Isolation and genetic manipulation of adult cardiac myocytes for confocal imaging. *J Vis Exp.* 2009; 31:e1433.
14. Louch WE, Sheehan KA, Wolska BM. Methods in cardiomyocyte isolation, culture, and gene transfer. *J Mol Cell Cardiol.* 2011; 51:288–298. DOI: 10.1016/j.yjmcc.2011.06.012 [PubMed: 21723873]
15. Graham EL, Balla C, Franchino H, Melman Y, del Monte F, Das S. Isolation, culture, and functional characterization of adult mouse cardiomyocytes. *J Vis Exp.* 2013; 79:e50289.
16. Roth GM, Bader DM, Pfaltzgraff ER. Isolation and physiological analysis of mouse cardiomyocytes. *J Vis Exp.* 2014; 91:e51109.
17. Li D, Wu J, Bai Y, Zhao X, Liu L. Isolation and culture of adult mouse cardiomyocytes for cell signaling and in vitro cardiac hypertrophy. *J Vis Exp.* 2014; 87:e51357.
18. Bai X, Fischer S, Keshavjee S, Liu M. Heparin interference with reverse transcriptase polymerase chain reaction of RNA extracted from lungs after ischemia-reperfusion. *Transpl Int.* 2000; 13:146–150. [PubMed: 10836652]

19. García ME, Blanco JL, Caballero J, Gargallo-Viola D. Anticoagulants interfere with PCR used to diagnose invasive aspergillosis. *J Clin Microbiol.* 2002; 40:1567–1568. [PubMed: 11923400]
20. Ghazalpour A, Rau CD, Farber CR, et al. Hybrid mouse diversity panel: a panel of inbred mouse strains suitable for analysis of complex genetic traits. *Mamm Genome.* 2012; 23:680–692. DOI: 10.1007/s00335-012-9411-5 [PubMed: 22892838]
21. Yue F, Cheng Y, Breschi A, et al. Mouse ENCODE Consortium. A comparative encyclopedia of DNA elements in the mouse genome. *Nature.* 2014; 515:355–364. DOI: 10.1038/nature13992 [PubMed: 25409824]
22. Dow LE, Fisher J, O'Rourke KP, Muley A, Kasthuber ER, Livshits G, Tschaharganeh DF, Succi ND, Lowe SW. Inducible in vivo genome editing with CRISPR-Cas9. *Nat Biotechnol.* 2015; 33:390–394. DOI: 10.1038/nbt.3155 [PubMed: 25690852]
23. Inagaki K, Fuess S, Storm TA, Gibson GA, Mctiernan CF, Kay MA, Nakai H. Robust systemic transduction with AAV9 vectors in mice: efficient global cardiac gene transfer superior to that of AAV8. *Mol Ther.* 2006; 14:45–53. DOI: 10.1016/j.ymthe.2006.03.014 [PubMed: 16713360]
24. Readnower RD, Brainard RE, Hill BG, Jones SP. Standardized bioenergetic profiling of adult mouse cardiomyocytes. *Physiol Genomics.* 2012; 44:1208–1213. DOI: 10.1152/physiolgenomics.00129.2012 [PubMed: 23092951]
25. Viero C, Kraushaar U, Ruppenthal S, Kaestner L, Lipp P. A primary culture system for sustained expression of a calcium sensor in preserved adult rat ventricular myocytes. *Cell Calcium.* 2008; 43:59–71. DOI: 10.1016/j.ceca.2007.04.001 [PubMed: 17822759]
26. Kramer JH, Chovan JP, Schaffer SW. Effect of taurine on calcium paradox and ischemic heart failure. *Am J Physiol.* 1981; 240:H238–H246. [PubMed: 6451184]
27. Piper HM, Probst I, Schwartz P, Hütter FJ, Spieckermann PG. Culturing of calcium stable adult cardiac myocytes. *J Mol Cell Cardiol.* 1982; 14:397–412. [PubMed: 7175947]
28. Volz A, Piper HM, Siegmund B, Schwartz P. Longevity of adult ventricular rat heart muscle cells in serum-free primary culture. *J Mol Cell Cardiol.* 1991; 23:161–173. [PubMed: 2067025]
29. Pinz I, Zhu M, Mende U, Ingwall JS. An improved isolation procedure for adult mouse cardiomyocytes. *Cell Biochem Biophys.* 2011; 61:93–101. DOI: 10.1007/s12013-011-9165-9 [PubMed: 21327944]
30. Leach RN, Desai JC, Orchard CH. Effect of cytoskeleton disruptors on L-type Ca channel distribution in rat ventricular myocytes. *Cell Calcium.* 2005; 38:515–526. DOI: 10.1016/j.ceca.2005.07.006 [PubMed: 16137761]
31. Hammer K, Ruppenthal S, Viero C, Scholz A, Edelmann L, Kaestner L, Lipp P. Remodelling of Ca<sup>2+</sup> handling organelles in adult rat ventricular myocytes during long term culture. *J Mol Cell Cardiol.* 2010; 49:427–437. DOI: 10.1016/j.yjmcc.2010.05.010 [PubMed: 20540947]
32. Kruppenbacher JP, May T, Eggers HJ, Piper HM. Cardiomyocytes of adult mice in long-term culture. *Naturwissenschaften.* 1993; 80:132–134. [PubMed: 8464521]
33. Hopkins WE, Chen Z, Fukagawa NK, Hall C, Knot HJ, LeWinter MM. Increased atrial and brain natriuretic peptides in adults with cyanotic congenital heart disease: enhanced understanding of the relationship between hypoxia and natriuretic peptide secretion. *Circulation.* 2004; 109:2872–2877. DOI: 10.1161/01.CIR.0000129305.25115.80 [PubMed: 15173030]
34. Vujic A, Robinson EL, Ito M, Haider S, Ackers-Johnson M, See K, Methner C, Figg N, Brien P, Roderick HL, Skepper J, et al. Experimental heart failure modelled by the cardiomyocyte-specific loss of an epigenome modifier, DNMT3B. *J Mol Cell Cardiol.* 2015; 82:174–183. DOI: 10.1016/j.yjmcc.2015.03.007 [PubMed: 25784084]
35. Guimarães-Camboa N, Stowe J, Aneas I, Sakabe N, Cattaneo P, Henderson L, Kilberg MS, Johnson RS, Chen J, McCulloch AD, Nobrega MA, et al. HIF1 $\alpha$  represses cell stress pathways to allow proliferation of hypoxic fetal cardiomyocytes. *Dev Cell.* 2015; 33:507–521. DOI: 10.1016/j.devcel.2015.04.021 [PubMed: 26028220]
36. Danziger RS, Sakai M, Lakatta EG, Hansford RG. Interactive alpha- and beta-adrenergic actions of norepinephrine in rat cardiac myocytes. *J Mol Cell Cardiol.* 1990; 22:111–123. [PubMed: 2157852]

37. Williams S, Pourrier M, McAfee D, Lin S, Fedida D. Ranolazine improves diastolic function in spontaneously hypertensive rats. *Am J Physiol Heart Circ Physiol.* 2014; 306:H867–H881. DOI: 10.1152/ajpheart.00704.2013 [PubMed: 24464752]
38. Despa S, Tucker AL, Bers DM. Phospholemman-mediated activation of Na/K-ATPase limits [Na]<sup>i</sup> and inotropic state during beta-adrenergic stimulation in mouse ventricular myocytes. *Circulation.* 2008; 117:1849–1855. DOI: 10.1161/CIRCULATIONAHA.107.754051 [PubMed: 18362230]
39. Chen KH, Xu XH, Sun HY, Du XL, Liu H, Yang L, Xiao GS, Wang Y, Jin MW, Li GR. Distinctive property and pharmacology of voltage-gated sodium current in rat atrial vs ventricular myocytes. *Heart Rhythm.* 2016; 13:762–770. DOI: 10.1016/j.hrthm.2015.11.022 [PubMed: 26598320]
40. Remme CA, Scicluna BP, Verkerk AO, et al. Genetically determined differences in sodium current characteristics modulate conduction disease severity in mice with cardiac sodium channelopathy. *Circ Res.* 2009; 104:1283–1292. DOI: 10.1161/CIRCRESAHA.109.194423 [PubMed: 19407241]
41. Johnson EA, Sommer JR. A strand of cardiac muscle. Its ultrastructure and the electrophysiological implications of its geometry. *J Cell Biol.* 1967; 33:103–129. [PubMed: 6033930]
42. Miller BA, Hoffman NE, Merali S, et al. TRPM2 channels protect against cardiac ischemia-reperfusion injury: role of mitochondria. *J Biol Chem.* 2014; 289:7615–7629. DOI: 10.1074/jbc.M113.533851 [PubMed: 24492610]
43. St Clair JR, Sharpe EJ, Proenza C. Culture and adenoviral infection of sinoatrial node myocytes from adult mice. *Am J Physiol Heart Circ Physiol.* 2015; 309:H490–H498. DOI: 10.1152/ajpheart.00068.2015 [PubMed: 26001410]
44. Wang D, Chang PS, Wang Z, Sutherland L, Richardson JA, Small E, Krieg PA, Olson EN. Activation of cardiac gene expression by myocardin, a transcriptional cofactor for serum response factor. *Cell.* 2001; 105:851–862. [PubMed: 11439182]
45. Xing W, Zhang TC, Cao D, Wang Z, Antos CL, Li S, Wang Y, Olson EN, Wang DZ. Myocardin induces cardiomyocyte hypertrophy. *Circ Res.* 2006; 98:1089–1097. DOI: 10.1161/01.RES.0000218781.23144.3e [PubMed: 16556869]
46. Howard CM, Baudino TA. Dynamic cell-cell and cell-ECM interactions in the heart. *J Mol Cell Cardiol.* 2014; 70:19–26. DOI: 10.1016/j.yjmcc.2013.10.006 [PubMed: 24140801]
47. Kamo T, Akazawa H, Komuro I. Cardiac nonmyocytes in the hub of cardiac hypertrophy. *Circ Res.* 2015; 117:89–98. DOI: 10.1161/CIRCRESAHA.117.305349 [PubMed: 26089366]
48. Smith AJ, Lewis FC, Aquila I, Waring CD, Nocera A, Agosti V, Nadal-Ginard B, Torella D, Ellison GM. Isolation and characterization of resident endogenous c-Kit<sup>+</sup> cardiac stem cells from the adult mouse and rat heart. *Nat Protoc.* 2014; 9:1662–1681. DOI: 10.1038/nprot.2014.113 [PubMed: 24945383]
49. Ali SR, Ranjbarvaziri S, Talkhabi M, Zhao P, Subat A, Hojjat A, Kamran P, Müller AM, Volz KS, Tang Z, Red-Horse K, et al. Developmental heterogeneity of cardiac fibroblasts does not predict pathological proliferation and activation. *Circ Res.* 2014; 115:625–635. DOI: 10.1161/CIRCRESAHA.115.303794 [PubMed: 25037571]
50. Furtado MB, Costa MW, Pranoto EA, Salimova E, Pinto AR, Lam NT, Park A, Snider P, Chandran A, Harvey RP, Boyd R, et al. Cardiogenic genes expressed in cardiac fibroblasts contribute to heart development and repair. *Circ Res.* 2014; 114:1422–1434. DOI: 10.1161/CIRCRESAHA.114.302530 [PubMed: 24650916]
51. Rust EM, Westfall MV, Metzger JM. Stability of the contractile assembly and Ca<sup>2+</sup>-activated tension in adenovirus infected adult cardiac myocytes. *Mol Cell Biochem.* 1998; 181:143–155. [PubMed: 9562251]
52. Guinamard R, Hof T, Sallé L. Current recordings at the single channel level in adult mammalian isolated cardiomyocytes. *Methods Mol Biol.* 2014; 1183:291–307. DOI: 10.1007/978-1-4939-1096-0\_19 [PubMed: 25023317]
53. Götz KR, Sprenger JU, Perera RK, Steinbrecher JH, Lehnart SE, Kuhn M, Gorelik J, Balligand JL, Nikolaev VO. Transgenic mice for realtime visualization of cGMP in intact adult cardiomyocytes. *Circ Res.* 2014; 114:1235–1245. DOI: 10.1161/CIRCRESAHA.114.302437 [PubMed: 24599804]

54. Kho C, Lee A, Jeong D, Oh JG, Gorski PA, Fish K, Sanchez R, DeVita RJ, Christensen G, Dahl R, Hajjar RJ. Small-molecule activation of SERCA2a SUMOylation for the treatment of heart failure. *Nat Commun.* 2015; 6:7229.doi: 10.1038/ncomms8229 [PubMed: 26068603]
55. Flynn JM, Santana LF, Melov S. Single cell transcriptional profiling of adult mouse cardiomyocytes. *J Vis Exp.* 2011; 58:e3302.
56. Roberge S, Roussel J, Andersson DC, Meli AC, Vidal B, Blandel F, Lanner JT, Le Guennec JY, Katz A, Westerblad H, Lacampagne A, et al. TNF- $\alpha$ -mediated caspase-8 activation induces ROS production and TRPM2 activation in adult ventricular myocytes. *Cardiovasc Res.* 2014; 103:90–99. DOI: 10.1093/cvr/cvu112 [PubMed: 24802330]
57. Crevey BJ, Langer GA, Frank JS. Role of Ca<sup>2+</sup> in maintenance of rabbit myocardial cell membrane structural and functional integrity. *J Mol Cell Cardiol.* 1978; 10:1081–1100. [PubMed: 745248]
58. Egorova MV, Afanas'ev SA, Popov SV. A simple method for isolation of cardiomyocytes from adult rat heart. *Bull Exp Biol Med.* 2005; 140:370–373. [PubMed: 16307061]
59. Wittenberg BA, White RL, Ginzberg RD, Spray DC. Effect of calcium on the dissociation of the mature rat heart into individual and paired myocytes: electrical properties of cell pairs. *Circ Res.* 1986; 59:143–150. [PubMed: 2427246]
60. Nair P, Nair RR. Selective use of calcium chelators enhances the yield of calcium-tolerant myocytes from adult heart. *Indian J Exp Biol.* 1997; 35:451–456. [PubMed: 9378512]
61. Scheuer J, Berry MN. Effect of alkalosis on glycolysis in the isolated rat heart. *Am J Physiol.* 1967; 213:1143–1148. [PubMed: 4228305]
62. Gannier F, White E, Lacampagne A, Garnier D, Le Guennec JY. Streptomycin reverses a large stretch induced increases in [Ca<sup>2+</sup>]<sub>i</sub> in isolated guinea pig ventricular myocytes. *Cardiovasc Res.* 1994; 28:1193–1198. [PubMed: 7954622]
63. Abi-Gerges N, Pointon A, Pullen GF, Morton MJ, Oldman KL, Armstrong D, Valentin JP, Pollard CE. Preservation of cardiomyocytes from the adult heart. *J Mol Cell Cardiol.* 2013; 64:108–119. DOI: 10.1016/j.yjmcc.2013.09.004 [PubMed: 24051370]
64. Kabaeva Z, Zhao M, Michele DE. Blebbistatin extends culture life of adult mouse cardiac myocytes and allows efficient and stable transgene expression. *Am J Physiol Heart Circ Physiol.* 2008; 294:H1667–H1674. DOI: 10.1152/ajpheart.01144.2007 [PubMed: 18296569]
65. Tian Q, Pahlavan S, Oleinikow K, Jung J, Ruppenthal S, Scholz A, Schumann C, Kraegeloh A, Oberhofer M, Lipp P, Kaestner L. Functional and morphological preservation of adult ventricular myocytes in culture by sub-micromolar cytochalasin D supplement. *J Mol Cell Cardiol.* 2012; 52:113–124. DOI: 10.1016/j.yjmcc.2011.09.001 [PubMed: 21930133]
66. Stapleton MT, Fuchsbauer CM, Allshire AP. BDM drives protein dephosphorylation and inhibits adenine nucleotide exchange in cardiomyocytes. *Am J Physiol.* 1998; 275:H1260–H1266. [PubMed: 9746474]
67. Ostap EM. 2,3-Butanedione monoxime (BDM) as a myosin inhibitor. *J Muscle Res Cell Motil.* 2002; 23:305–308. [PubMed: 12630704]
68. Gwathmey JK, Hajjar RJ, Solaro RJ. Contractile deactivation and uncoupling of crossbridges. Effects of 2,3-butanedione monoxime on mammalian myocardium. *Circ Res.* 1991; 69:1280–1292. [PubMed: 1934358]

## Novelty and Significance

### What Is Known?

- Isolation of healthy, intact cardiac myocytes from the mouse heart is challenging and a barrier to progress in cardiac research.
- Current established protocols rely on the use of Langendorff apparatus, which requires considerable technical expertise.

### What New Information Does This Article Contribute?

- We describe a convenient, alternative approach, using direct needle perfusion of the left ventricle *ex vivo*, allowing the robust isolation and culture of adult mouse cardiac myocytes using only common surgical and laboratory equipment.
- Myocytes are isolated with yields, viability, and functionality comparable to those in published Langendorff-based methods.
- The technique also permits concurrent isolation, separation, and coculture of nonmyocyte cardiac cell populations.
- Progress in cardiac research is hampered by unique complexities associated with the isolation of viable myocytes from the adult mouse heart. Current protocols rely on reverse aortic perfusion using specialized Langendorff apparatus, which poses considerable logistical and technical barriers to researchers and demands extensive training. We therefore sought to validate an alternative, simplified approach. Our protocol achieves yields of myocytes comparable to those in published Langendorff-based methods, by direct needle perfusion of the left ventricle *ex vivo*, using only common surgical and laboratory equipment. Isolated myocytes are viable, functional, and amenable to a full range of investigative techniques. Furthermore, the methodology permits concurrent isolation, separation, and coculture of myocyte and nonmyocyte cardiac populations, including fibroblasts and endothelial cells. We anticipate that this new approach will expand and accelerate innovative research in the field of cardiac biology.



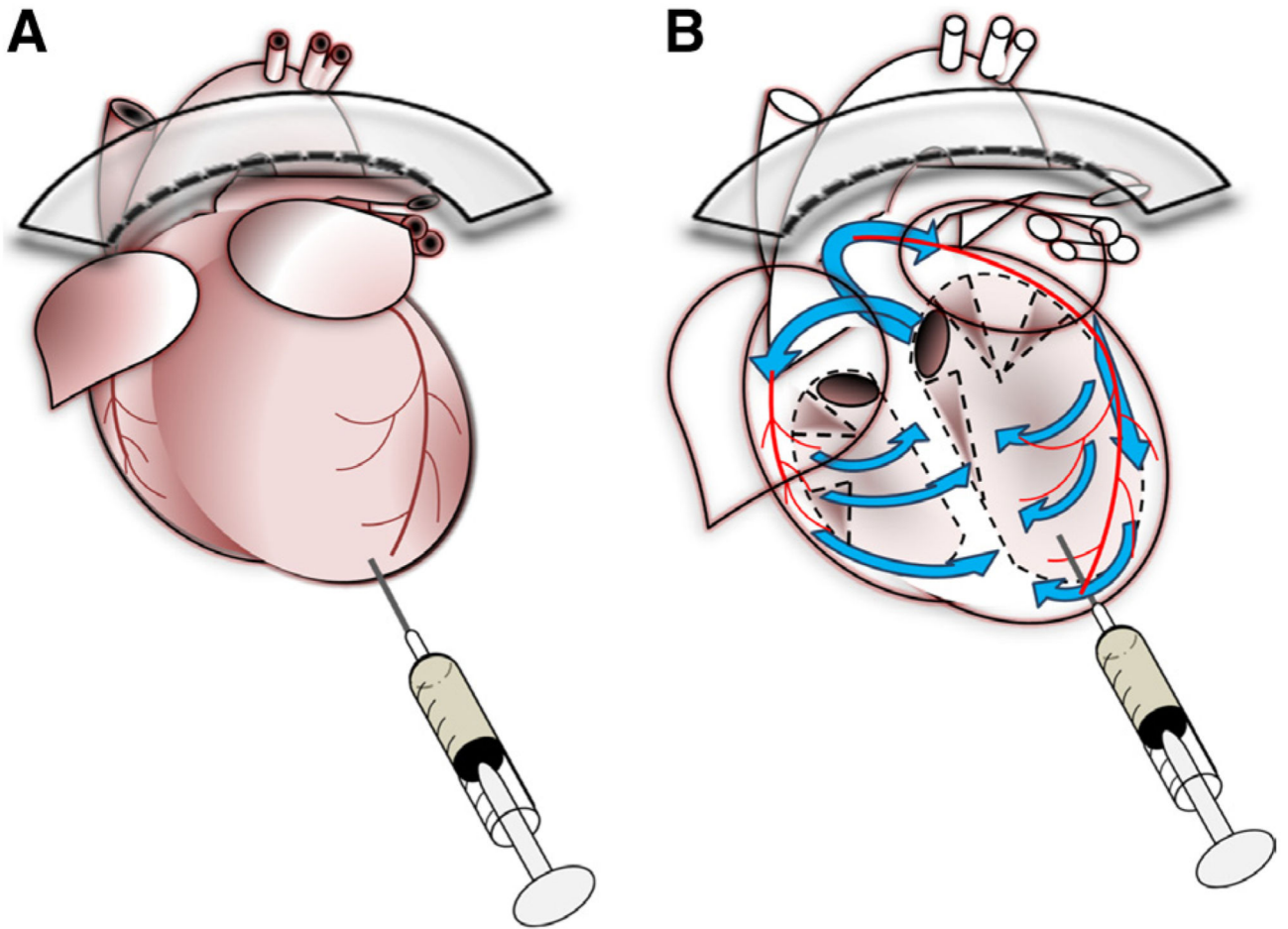
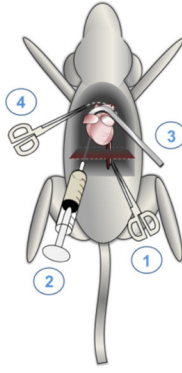
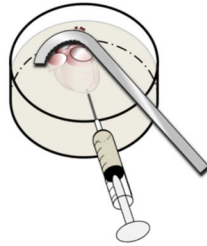


**Figure 1. A new method to isolate cardiac myocytes from the adult mouse heart.** Schematic diagrams illustrating the principle of the approach, in which traditional Langendorff-based retrograde aortic perfusion is replaced by simple injection of dissociation buffers into the left ventricle (**A**). Application of a hemostatic aortic clamp forces passage of buffers (blue arrows; **B**) through the coronary circulation (red), ensuring deep perfusion of the myocardium.



Chest cavity of anaesthetised mouse is opened to below diaphragm (red) to fully expose heart.

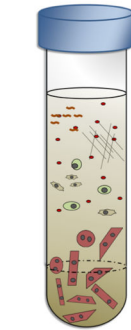
- (1) Descending aorta and inferior vena cava are cut.
- (2) 7 ml EDTA buffer is injected into apex of right ventricle.
- (3) Lahey forceps reach behind heart to clamp aorta.
- (4) Heart is removed by cutting behind clamp.



Clamped heart is submerged in 60 mm dish of EDTA buffer. 10 ml EDTA buffer is injected into apex of left ventricle (LV).



Heart is transferred to dish of perfusion buffer. 3 ml perfusion buffer is injected into apex of LV.



Heart is transferred to dish of collagenase buffer. 30-40 ml collagenase buffer injected into apex of LV, until digestion is apparent.

Clamp is removed. Heart may be separated into respective chambers as desired. Tissue is then pulled gently into ~1mm<sup>3</sup> pieces using forceps, and dissociated by gentle pipetting.

Stop buffer is added. Cell suspension is passed through 100 µm strainer and myocytes gravity settle for 20 min.

Supernatant containing non-myocyte cells, debris and extracellular matrix is collected. Myocytes then undergo two further rounds of gravity settling to achieve a pure population that may be harvested, applied in acute studies, or plated for in vitro culture.

Similarly, supernatant fractions are combined and centrifuged to isolate non-myocyte populations.

**Figure 2. Summary of the cardiac myocyte isolation protocol.**

A detailed, extended description of methodology, with images and video, is available in the Online Data Supplement. LV indicates left ventricle.

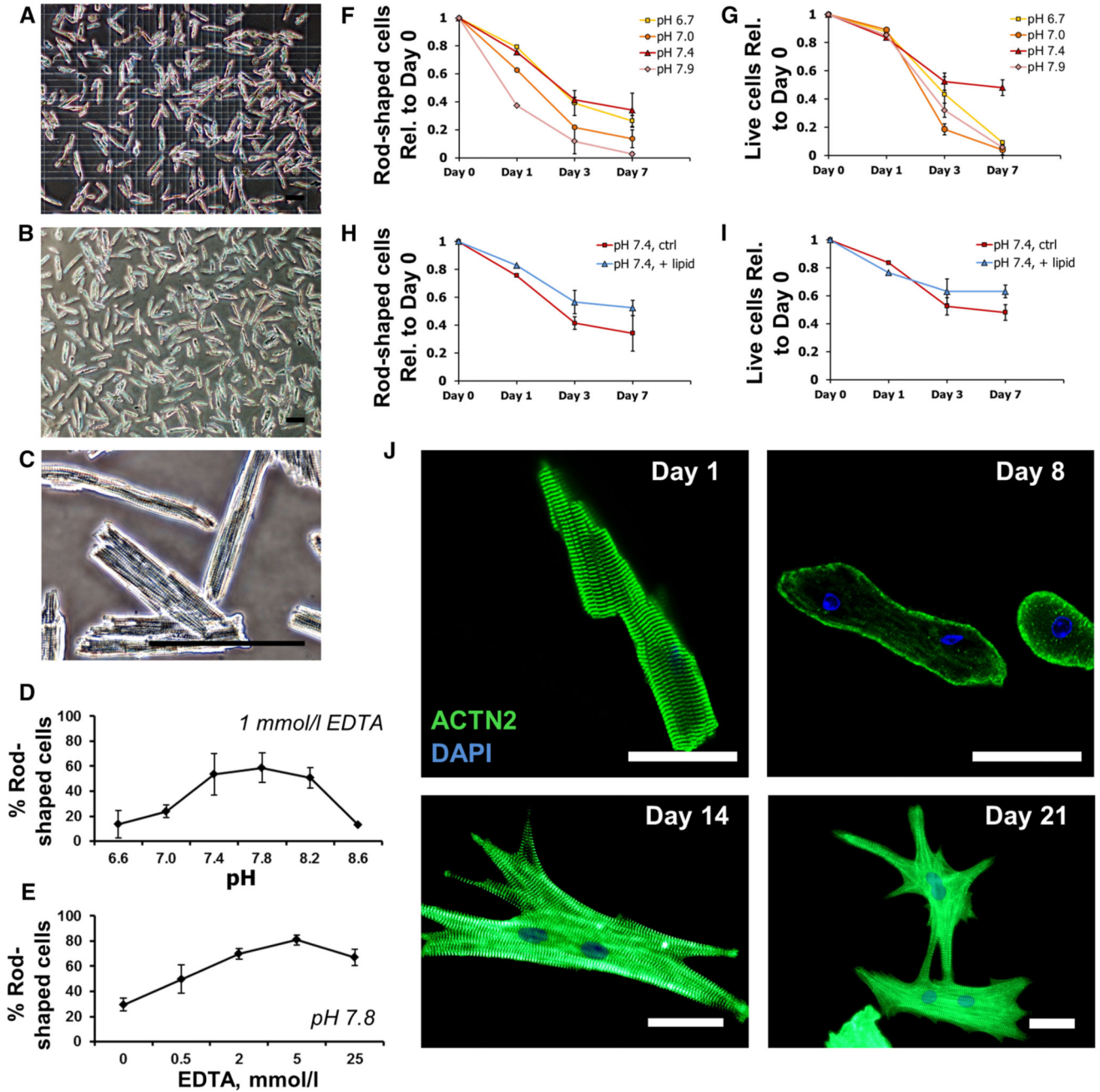


**Figure 3. Protocol optimization and isolation of high yields of viable cardiac myocytes.**

**A–C**, Representative images of adult mouse left ventricular digestion products, before plating (**A**), and after 1-h culture (**B** and **C**), showing yields of 80% rod-shaped, viable myocytes, with organized sarcomeric striations. Scale bars=100  $\mu$ m. **D**, Optimization of dissociation buffer pH. Highest viable yields were obtained at pH 7.8. EDTA concentration was 1 mmol/L. **E**, Optimization of EDTA concentration. Highest yields were obtained at 5 mmol/L EDTA. Buffer pH was 7.8. Data show mean $\pm$ SD, n=3 independent experiments. **F–I**, Quantification of myocyte rod shape morphology (**F** and **H**) and viability (exclusion of

ethidium homodimer stain, **G** and **I**) for a time course of 7 d in culture at specified pH range (**F** and **G**) and with or without lipid supplementation at optimal pH 7.4 (**H** and **I**), as indicated. Data show mean±SD, n=2 independent experiments in biological triplicate. **J**, Immunologic staining and confocal imaging of myocytes with sarcomeric- $\alpha$ -actinin antibody (ACTN2; green) and DAPI (4',6-diamidino-2-phenylindole), after increasing time in culture, as indicated. Loss of sarcomeric organization was observed after 8-d culture. 10% fetal bovine serum was included in cultures from day 8 onward, and 2,3-butanedione monoxime removed. Extended culture resulted in re-establishment of sarcomeric structures, formation of cell–cell contacts, and synchronized, spontaneous contractility. Scale bars=50  $\mu$ m.

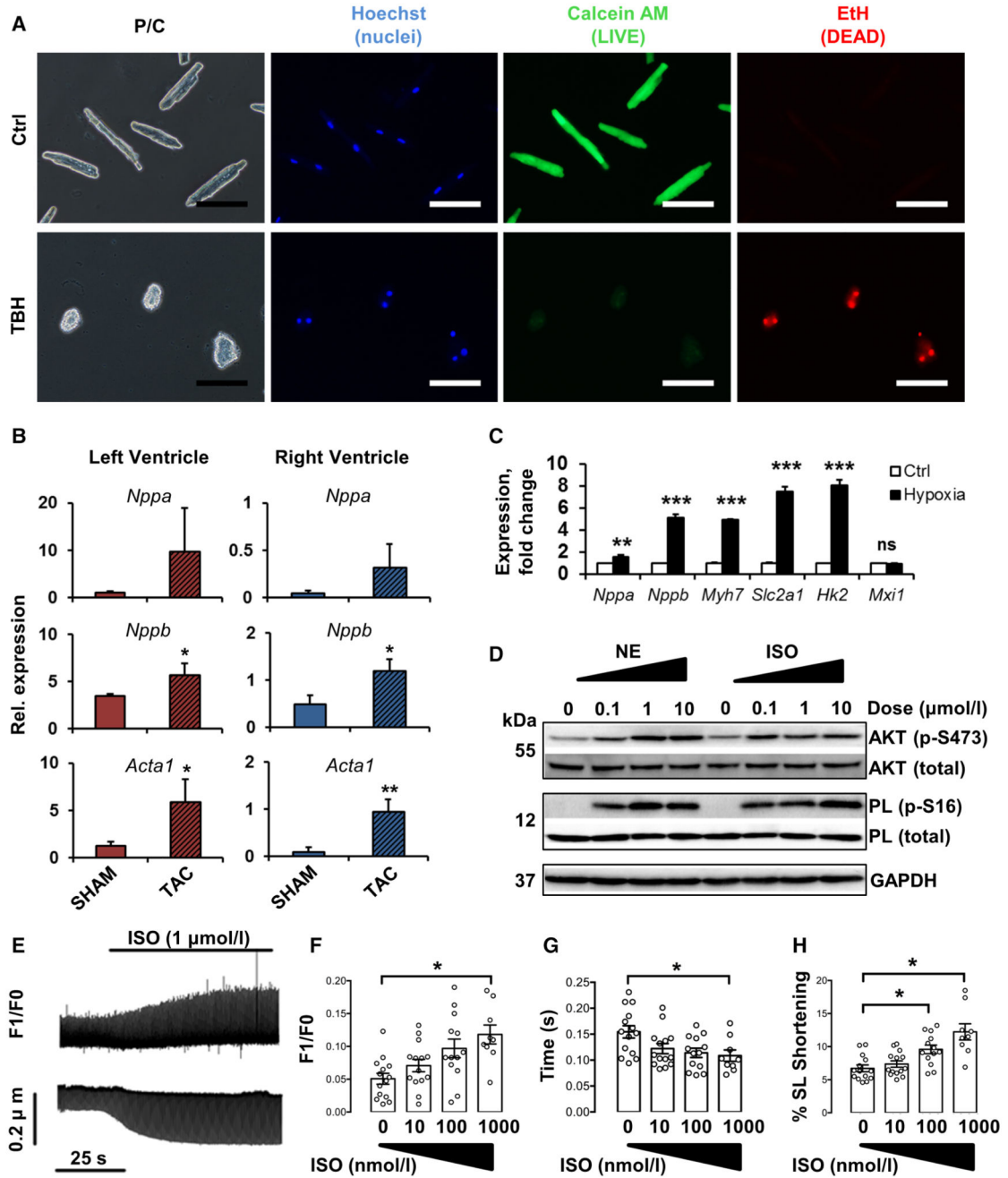


**Figure 4. Cultured cardiac myocytes retain transcriptional and functional characteristics and are amenable to investigation.**

**A**, Isolated myocytes are viable with intact plasma membranes. Freshly plated myocytes retain calcein (green) but exclude ethidium (EtH, red). Addition of 10  $\mu\text{mol/L}$  butyl-peroxide (TBH) led to calcein escape and entry of EtH. Nuclear counterstain, Hoechst-33342. Scale bars=100  $\mu\text{m}$ . **B**, Myocytes from both ventricles retain characteristic transcriptional signatures after isolation from a pressure-overload model of hypertrophy (TAC), compared with sham-operated controls. Expression was quantified by quantitative polymerase chain

reaction, relative to *18S*. Data show mean±SD, n=3 mice per group. \* $P<0.05$ , \*\* $P<0.01$ , Student *t* test. **C**, Hypoxia-regulated genes *Nppa*, *Nppa*, *Myh7*, *Slc2a1*, and *Hk2*, but not *Mxi1*, were significantly upregulated in cultured myocytes after 24-h hypoxic exposure. Data show mean±SD, n=3 independent experiments, expression relative to *18S*. \*\* $P<0.01$ , \*\*\* $P<0.001$ , Student *t* test. **D–H**, Myocytes are responsive to adrenergic stimulation in a dose-dependent manner. **D**, Western blot to demonstrate phosphorylation of AKT and phospholamban (PL), 20 min after addition of norepinephrine (NE) or isoproterenol (ISO), as indicated. **E–H**, Myocytes were loaded with fura2-AM and paced at 2 Hz in the presence of ISO as indicated. Calcium transients and sarcomere length shortening were measured using the integrated photometry/contractility system (Ionoptix). **E**, Representative raw traces of calcium transients (**upper**) and sarcomere length (**lower**) recorded from a single cell, ISO added as indicated. Calcium transient amplitude (**F**), calcium transient decay (**G**), and % sarcomere length (SL) shortening (**H**) were subsequently quantified in response to ISO addition as indicated. Data show mean±SE, n = 9 cells from 3 hearts, \* $P<0.05$ , 1-way ANOVA followed by Dunnett multiple comparisons test.

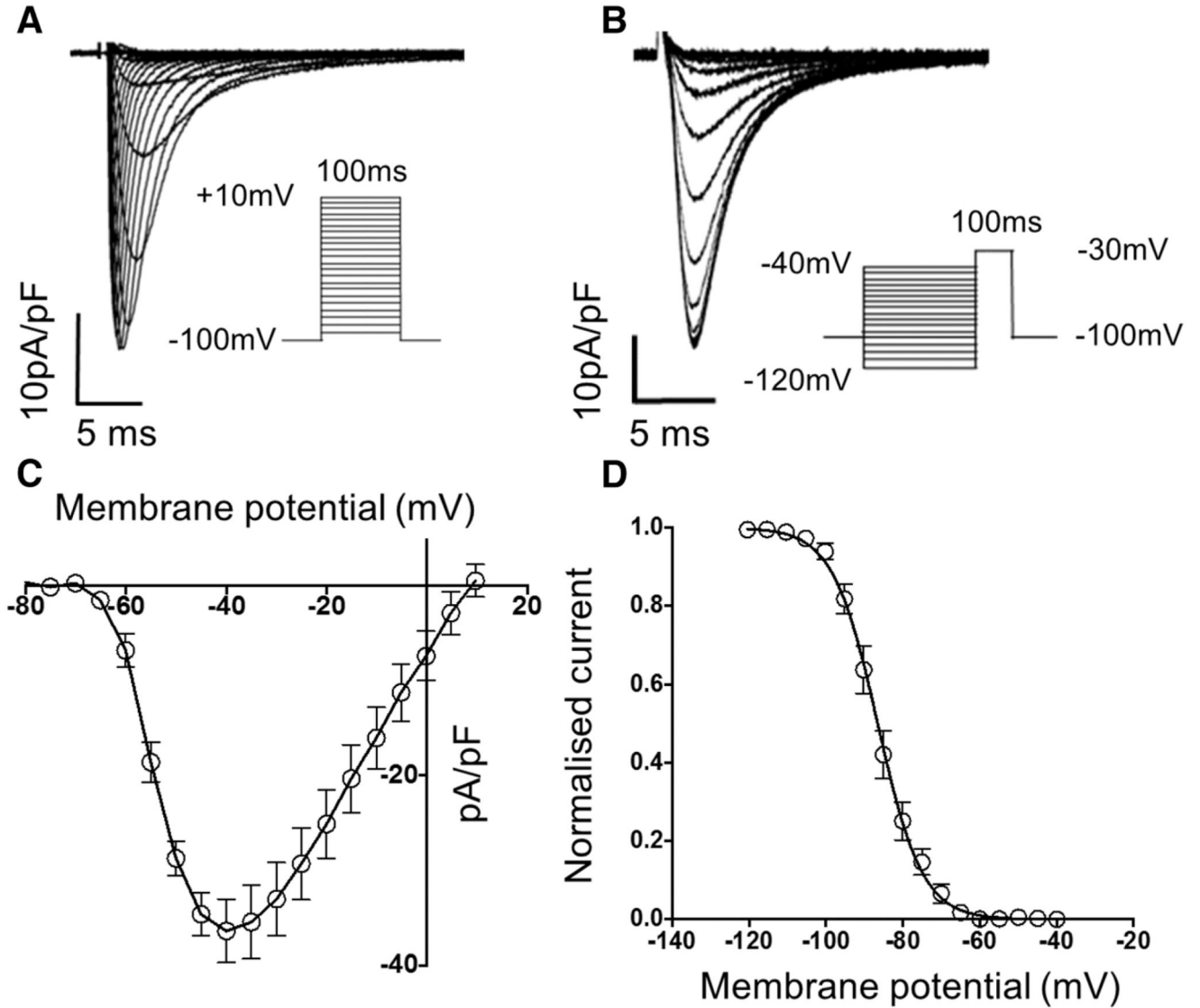


**Figure 5. Isolated myocytes display normal sodium currents ( $I_{Na}$ ).**

$I_{Na}$  were measured in freshly isolated left ventricular cardiac myocytes. **A**, Representative voltage-dependent  $I_{Na}$  raw traces recorded from a single ventricular cardiac myocyte. The voltage protocol is shown in the inset. **B**, Mean data for current–voltage relationship of  $I_{Na}$  current density (pA/pF;  $n=8$  cells from 3 hearts). **C**, Representative raw traces showing voltage-dependent steady-state  $I_{Na}$  inactivation. The voltage protocol is shown in the inset. **D**, Mean data for  $I_{Na}$  inactivation curve ( $n=8$  cells from 3 hearts).

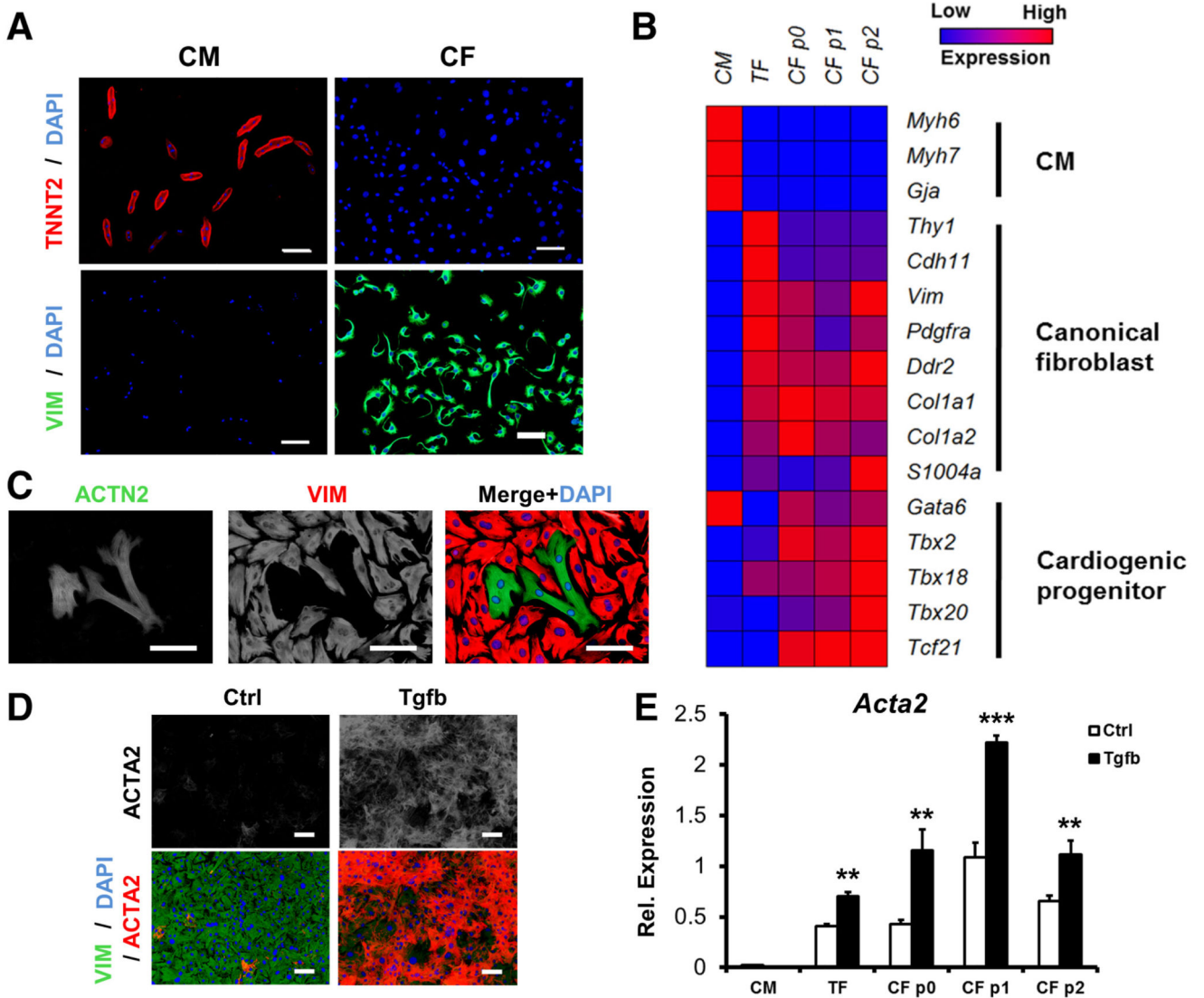


**Figure 6. Concomitant culture and study of cardiac myocytes and fibroblasts from the same mouse heart.**

**A**, Immunologic staining of isolated cardiac myocytes (CM) and cardiac fibroblasts (CF) with cardiac troponin-T antibody (TNNT2, red), vimentin antibody (VIM, green), and DAPI (4',6-diamidino-2-phenylindole), after 3-d culture. Specific staining demonstrates strong separation of myocyte and nonmyocyte fractions. **B**, Transcriptional analysis of cultured CM, tail fibroblasts (TF), and CF after 3-d culture, and CF after 1 (p1) or 2 (p2) passages in culture. Expression of selected cardiac myocyte-related (CM), canonical fibroblast-related, and cardiogenic-related genes was determined by quantitative polymerase chain reaction, relative to *18S*, and presented in heat map format. Data represent mean expression, n=2 independent experiments in biological triplicate. **C**, Coculture of cardiac myocytes and fibroblasts from the same mouse heart. Cell fractions were isolated, recombined after 3-d separate culture, and maintained for 4 further days in the presence of 10% fetal bovine serum. Cells were fixed and costained with antibodies against sarcomeric- $\alpha$ -actinin



(ACTN2, green, CM), vimentin (VIM, red, CF), and DAPI. **D**, Activation of isolated CFs after 24-h incubation with 10 ng/mL transforming growth factor beta (Tgfb) was detected by immunologic staining for smooth muscle  $\alpha$ -actin (ACTA2) production. **E**, The potential for activation of isolated CFs with Tgfb persisted for at least 2 passages. Data show mean $\pm$ SD, n=2 independent experiments in biological triplicate, *Acta2* expression relative to *18S*. \*\* $P<0.01$ , \*\*\* $P<0.001$ , Student *t* test, compared with relevant unstimulated controls.

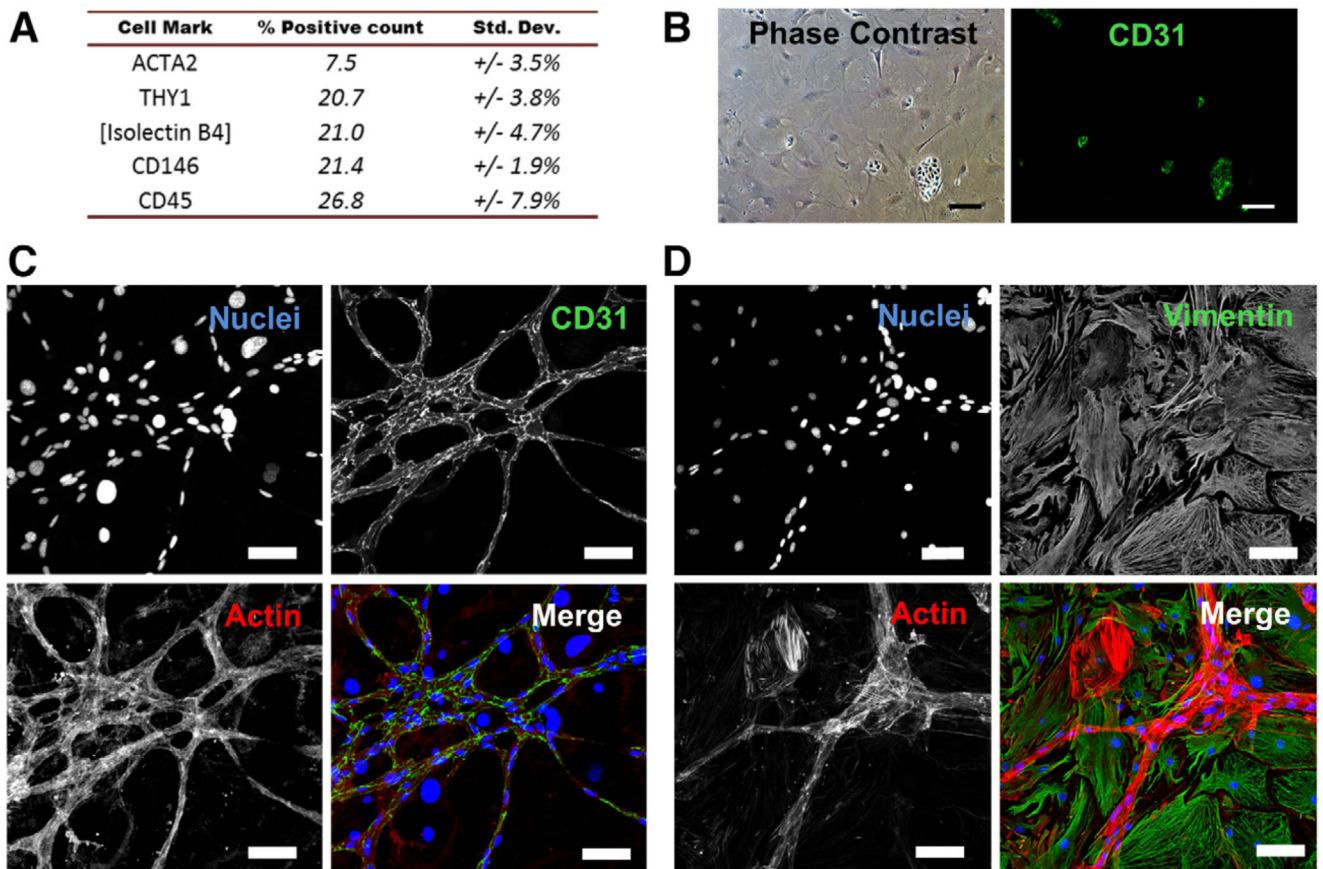


**Figure 7. Isolated cardiac nonmyocytes represent a heterogeneous population.**

**A**, Relative proportions of nonmyocyte fraction cells detected positive for putative identity markers: ACTA2 (smooth muscle), THY1 (cardiac fibroblast), CD146, GSL-Isolectin-B4 (endothelial), and CD45 (immunocyte), by flow cytometry. Data averaged from 3 independent experiments. **B**, Immunologic staining of CD31 (PECAM-1) in subconfluent nonmyocyte fraction cultures marked clusters of endothelial-like cells (green). **C** and **D**, In postconfluent cultures, these cells were observed to form CD31-positive (green), actin-rich (stained using fluorophore-conjugated phalloidin; red) networks (**C**) that stained negative for the fibroblast marker vimentin (VIM; green; **D**). All scale bars=100  $\mu$ m.